Journal of Crystal Growth 311 (2009) 1021–1024

Contents lists available at ScienceDirect

Journal of Crystal Growth

journal homepage: www.elsevier.com/locate/jcrysgro

# Epitaxially strained $Na_{0.7}CoO_2$ thin films on $SrTiO_3$ buffer layer

J.Y. Son, Y.-H. Shin, Hyungjun Kim *

*Department of Materials Science and Engineering, Pohang University of Science and Technology (POSTECH), Pohang 790-784, Republic of Korea*

ARTICLE INFO

*Article history:*
Received 20 October 2008
Received in revised form
17 November 2008
Accepted 20 November 2008
Communicated by M. Kawasaki
Available online 25 November 2008

*PACS:*
61.05.cp
71.30.+h
72.15.−v

*Keywords:*
A1. Crystal structure
A1. X-ray diffration
A3. Laser epitaxy
B1. Oxides

ABSTRACT

We prepared $Na_{0.7}CoO_2$ thin films on (0 0 1) $Al_2O_3$ substrates that showed a negligibly strained structure and a metallic behavior similar to $Na_{0.7}CoO_2$ single crystal. In particular, a $Na_{0.7}CoO_2$ thin film on a (1 1 1) $SrTiO_3$/(0 0 1) $Al_2O_3$ substrate exhibited an elongated *c*-lattice constant as well as an anomaly in the electric transporting behavior: a transition from an insulating state to a metallic state at 105 K. This change is caused by the structural symmetry break near the cubic-to-tetragonal transition temperature of $SrTiO_3$. From spectroscopic ellipsometry analysis, we obtained optical conductivities for the $Na_{0.7}CoO_2$ thin films on the $Al_2O_3$ and $SrTiO_3/Al_2O_3$ substrates. The $Na_{0.7}CoO_2$ thin film on the $SrTiO_3/Al_2O_3$ substrate exhibited higher energy splitting between $e_g$ and $a_{1g}$ than the $Na_{0.7}CoO_2$ thin film on the $Al_2O_3$ substrate, resulting from the *c*-lattice elongation.



## 1. Introduction

Sodium cobalt oxide $Na_xCoO_2$ has been attractively researched due to its large thermoelectric power and low resistivity for various thermoelectric applications [1]. In $Na_xCoO_2$, large thermoelectric power is attributed to spin entropy in a low-spin state of Co ion [2]. Many theoretical and experimental interests were triggered by superconductivity of $Na_{0.35}CoO_2 \cdot 1.3H_2O$, rich phase diagrams of $Na_xCoO_2$ with respect to *x*, and novel ground states induced by two-dimensional transition-metal oxide triangular lattice [3–5]. In addition, $Na_xCoO_2$ depending on the sodium content *x* exhibited complicated metallic transport behaviors with various magnetic orderings of paramagnetic metal, "Cure–Weiss" metal (anitiferromagnetic ordering), and spin-density wave (SDW) metal except a charge ordering state of anitiferromagnetic ordering [6,7]. Behind the rich physical properties, two-dimensional triangular lattice and mixed valence character led to puzzling ground states [6,7].

The crystal structure of $Na_xCoO_2$ consists of two-dimensional triangular $CoO_2$ layers of edge-sharing $CoO_6$ octahedrons separated by an insulating layer of $Na^+$ ions. There are four known phases of α-, α′-, β-, and γ-distinguished by the stacking orders of $CoO_2$ layers and the concentrations of Na ions [8]. A β-phase has a monoclinic unit cell with a space group symmetry of C2/m and lattice constants of $a$=4.90, $b$=2.83, $c$=5.72 Å, and $\beta$=105.96° and a γ-phase has a hexagonal structure with a space group symmetry of $P6_3/mmc$ and lattice constants of $a$=2.84 and $c$=10.81 Å [9,10]. In γ-$Na_xCoO_2$, the in-plane directions of $CoO_6$ octahedra along the out-of-plane direction of $CoO_2$ layers are alternating with the type of A–B, B–A, A–B, etc. where A and B are oxygen layers. These structural varieties of $Na_xCoO_2$ imply that the bulk modulus along the in-plane direction is small and the stress generated by lattice misfit is an important parameter for the growth of epitaxial thin films because of various possible stacking structures of $CoO_2$ layers and the possibility of the stacking fault.

Physical properties obtained from $Na_xCoO_2$ single crystals and powders have been widely researched but there have been a few reports about thin film studies [11–13]. From the standing point of the strain effect, thin film growth can give an opportunity for a manipulation of physical properties by changing stress using different substrates and growth parameters (substrate temperatures, oxygen partial pressures, etc.). We controlled structures of $Na_xCoO_2$ thin films from a β-phase with an island growth mode to a γ-phase with a layer-by-layer growth mode by varying a deposition rate [11]. In this study, we report the strain effect on electrical transport properties of epitaxial $Na_{0.7}CoO_2$ thin films deposited on $Al_2O_3$ and (1 1 1) $SrTiO_3/Al_2O_3$ substrates.

*Corresponding author. Tel.: +82 54 279 5409; fax: +82 54 279 2399.
*E-mail address:* hyungjun@postech.ac.kr (H. Kim).

0022-0248/$ - see front matter © 2008 Elsevier B.V. All rights reserved.
doi:10.1016/j.jcrysgro.2008.11.072

## 2. Experimental details

$Na_{0.7}CoO_2$ thin films were deposited on (0 0 1) $Al_2O_3$ substrates and (1 1 1) $SrTiO_3/Al_2O_3$ substrates by an eclipse pulsed laser deposition (PLD) method. In eclipse PLD, a deposition rate and energies of adatoms simultaneously reduce because high-energy particles are directly screened by a shadow mask. There is a lattice misfit of 2.9% between *c*-oriented $Na_{0.7}CoO_2$ and (0 0 1) $Al_2O_3$, which induces a compressive stress. A $Na_{0.8}CoO_2$ target was prepared by a conventional solid-state reaction method [11]. A commercially available 1 in $SrTiO_3$ target was used for the fabrication of a $SrTiO_3$ buffer layer on a (0 0 1) $Al_2O_3$ substrate. A frequency tripled (355 nm, ~2 J/cm$^2$) Nd:YAG laser was used for the deposition, and the distance between the target and the substrate was ~4 cm. For the deposition of $SrTiO_3$ buffer layers, we used a substrate temperature of 800 °C and an oxygen partial pressure of 200 m Torr. For the deposition of $Na_{0.7}CoO_2$ thin films, the optimum substrate temperature was 480 °C and the optimum partial oxygen pressure was 400 m Torr [11]. On (0 0 1) $Al_2O_3$ substrates, γ-$Na_{0.7}CoO_2$ thin films with a layer-by-layer growth mode were grown by using a low deposition rate of 0.02 Å/pulse.

The thickness of the $Na_{0.7}CoO_2$ thin films and the thickness of the $SrTiO_3$ buffer layers were, respectively, ~1000 and ~500 Å determined from cross-sectional scanning electron microscope (SEM) images. Tentative compositions of $Na_{0.7}CoO_2$ thin films were confirmed by energy dispersive X-ray spectrometer (EDS). For structural analysis, X-ray diffraction (XRD) data were obtained by a conventional laboratory X-ray diffractometer (CuKα1 radiation, 1.540 Å). Surface morphologies and topographies of $Na_{0.7}CoO_2$ thin films were observed by scanning probe microscope (SEM) and atomic force microscope (AFM). Temperature dependence of resistivity was measured in the temperature range 6–350 K. We analyzed spectroscopic ellipsometry data with an incident angle of 70° by a multi-wavelength variable-angle ellipsometer (J.A. Woollam Co.). At the energy range of 0.7–6.0 eV, ellipsometry parameters of $\Psi$ and $\Delta$ were measured and these parameters are defined by $R_\rho/R_s=\tan\Psi\exp(i\Delta)$, where $R_\rho$ and $R_s$ are complex reflection coefficients for the polarized light in parallel and perpendicular to the plane of incidence, respectively. Based on a Levenberg–Marquardt Algorithm, we fit $\Psi'$ and $\Delta'$ for a model of $Na_{0.7}CoO_2$ thin films to experimental parameters of $\Psi$ and $\Delta$.

## 3. Results and discussion

Fig. 1(a) shows the XRD pattern of the $Na_{0.7}CoO_2$ thin film on the (0 0 1) $Al_2O_3$ substrate. For the (0 0 2) peak, the full-width at half-maximum (FWHM) of the rocking curve was about 0.8°. The *c*-lattice constant of 10.8 Å was obtained from the 2$\theta$ values of the (0 0 2) and (0 0 4) peaks, which agrees well with the experiment for the variation of *c*-lattice constants depending on Na concentration [4]. To check an in-plane crystalline structure, we performed Φ-scans. Fig. 1(b) shows Φ-scans for the (1 0 4) peaks of the epitaxial $Na_{0.7}CoO_2$ thin film and the (1 0 4) peaks of the (0 0 1) $Al_2O_3$ substrate. The six-fold symmetry of the (1 0 4) peak represents a hexagonal structure of the $Na_{0.7}CoO_2$ thin film with twinning. The FWHM of an in-plane (1 0 4) peak for a $\theta-2\theta$ scan was about 0.55°. From the 2$\theta$ value of the (1 0 4) peak, we obtained a hexagonal *a*-axis constant of 2.8 Å.

In order to modify lattice misfit, we used a (1 1 1) $SrTiO_3$ buffer layer between a $Na_{0.7}CoO_2$ thin film and an $Al_2O_3$ substrate. A $SrTiO_3$ buffer layer can give a lattice misfit in the range 2.4–2.9%. Fig. 2(a) shows the XRD pattern of the $Na_{0.7}CoO_2$ thin film on the (1 1 1) $SrTiO_3/Al_2O_3$ substrate. For the (0 0 2) peak, the FWHM of the rocking curve was about 0.9° which is larger than 0.8° of the $Na_{0.7}CoO_2$ thin film on the (0 0 1) $Al_2O_3$ substrate. From the 2$\theta$ value of the (0 0 2) peak, the *c*-lattice constant of 11.4 Å was obtained and this *c*-lattice constant is larger than that of the $Na_{0.7}CoO_2$ thin film on (0 0 1) $Al_2O_3$ substrate. This elongation of the *c*-lattice constant indicates that the $Na_{0.7}CoO_2$ thin film adequately released a stress induced from the lattice misfit.

Fig. 2(b) shows Φ-scans of the (1 0 4) peaks of the epitaxial $Na_{0.7}CoO_2$ thin film, the (1 0 4) peaks of the $SrTiO_3$ buffer layer, and the (1 0 4) peaks of the $SrTiO_3/Al_2O_3$ substrate. The $SrTiO_3$ buffer layer and the $Na_{0.7}CoO_2$ thin film have six-fold symmetry with twinning. The FWHM of the in-plane (2 0 1) peak of the $Na_{0.7}CoO_2$ thin film is about 1.25° and this FWHM value is also lager than that of the $Na_{0.7}CoO_2$ thin film on the (0 0 1) $Al_2O_3$ substrate. From the 2$\theta$ value of the (1 0 4) peak, a hexagonal *a*-axis constant of 2.8 Å was obtained. Consequently, the $Na_{0.7}CoO_2$ thin film on the (1 1 1) $SrTiO_3/Al_2O_3$ substrate has a larger strain than the $Na_{0.7}CoO_2$ thin film on the (0 0 1) $Al_2O_3$ substrate.

We observed spiral patterns with multi-terraces in the AFM image of the $Na_{0.7}CoO_2$ thin film on the (1 1 1) $SrTiO_3/Al_2O_3$ substrate (not shown). The terrace heights were close to the *c*-lattice constant. The terrace width of ~100 nm was observed, indicating that the thin film had an atomically flat surface. Moreover, this large width of the terraces represents that surface diffusion lengths of adatoms are quite long and kinetics of steps is widespread [13]. The root mean square (RMS) surface roughness was about 1.0 nm.

Fig. 3 shows the temperature dependence of resistivities for the $Na_{0.7}CoO_2$ thin films on the (0 0 1) $Al_2O_3$ and (1 1 1) $SrTiO_3/Al_2O_3$ substrates. The resistivity of the $Na_{0.7}CoO_2$ thin film on the (0 0 1) $Al_2O_3$ substrate shows a metallic behavior similar to the

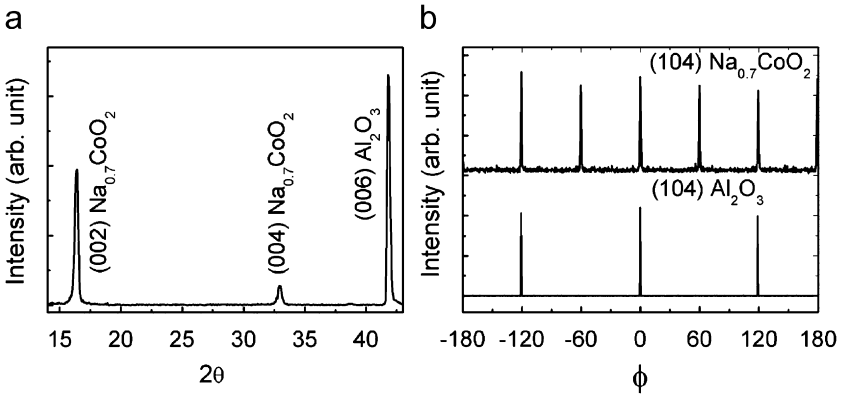


**Fig. 1.** (a) The XRD pattern of the epitaxial $Na_{0.7}CoO_2$ thin film on the (0 0 1) $Al_2O_3$ substrate. (b) The Φ-scans of the (1 0 4) peaks of the epitaxial $Na_{0.7}CoO_2$ thin film and the (1 0 4) peaks of the (0 0 1) $Al_2O_3$ substrate.